

Investigation of Different Geometrics of an Air-Cooled Heat Sink for Temperature Reduction by Using Finite Element Analysis

Patrick Petzka*¹, Tien – Dat Hoang¹

*Mechanical Engineering Department, University of Magdeburg, Germany¹ Faculty of International Training, Thai Nguyen University of Technology, Vietnam

ABSTRACT:- In the following study, the optimal geometry for an air-cooled heat sink of a 3D printer head was investigated, whereby the temperature in the inner area should be minimized. It has been seen that a maximal surface through a high number of fins is advantageous. The accumulation of material for a better heat conduction from the critical area has no essential influence on the cooling properties.

Keywords: Heat sink, Heat-break, 3D printer head, Fused Deposition Modeling, Finite element analysis, Radiation, Conduction

I. INTRODUCTION

Problem In the printer head of 3D printers, which are working according to the principle of Fused Deposition Modeling (FDM) the material must achieve a temperature of 240°C [1]. In this way the material has a viscous condition. Thus, the part can be created layer by layer. However, the material should not be melting in the feed system otherwise the feed stop or rather the feed rate is not constant. Therefore, the material is air-cooled by a heat sink above the heat-break (Fig. 1). The better the air-cooled heat sink works the lower is the probability that the material will stick on the inner side of the pipe into the heat sink.

Task

In this study the geometrical dimensions of a commercial heat sink should vary, so that there is a minimal temperature on the inner side of the heat sink. The external shape and the choice of material should be constant. The thermal behavior of the heat sink will be in progress with finite elements simulation program Ansys Workbench R14.5.

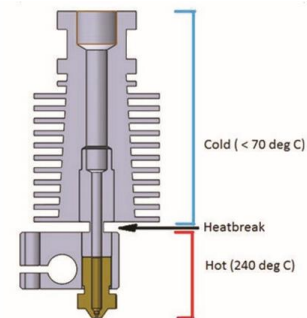


Fig. 1 Heating area and cooling area of the printer head [1]

II. STATE OF THE ART ADDITIVE MANUFACTURING

The additive manufacturing (AM) describes a process which enables to accumulate materials in layers until the part is produced on the basis of digital design data [2] (standardized in ISO/TC 261). Thus, there are following benefits in comparison to conventional and subtractive manufacturing. Besides the universally usable 3D printer with no additional tools are required. So you can save money and time for tools, manufacturing molds and make-ready times. Furthermore, you have a location-independent production of products. Undercuts and cavities do not need to be considered separately. Through the layer-by-layer buildup of the parts, materials can be omitted in unnecessary areas. So you can save material and have a lightweight construction. AM has the disadvantage, that they are ineffective by high quantities per time unit in comparison to conventional methods. Furthermore, the surface of AM products needs a post-production to comply the required tolerances of surfaces [3]. The AM of parts can be realized by following different procedures. By applying the Selective Laser Sintering (SLS) and the Selective Laser Melting (SLM) a material powder is melted locally by a laser or electron beam. This melted material combines with the already sintered basic material. By applying the Stereolithography (STL) and Polyjet Technique a local co-polymerization is initiated by ultra-violet light. This leads to a solidification of the material. By using 3D printing based on binder-Technology (3DP) a binder is applied locally on a powder board. Afterward a new powder layer is created. This process is repeatable. Another procedure is the Laminated Object Manufacturing (LOM). The paper is combined by glue and the mold is finally generated by cutting a profile section [4].

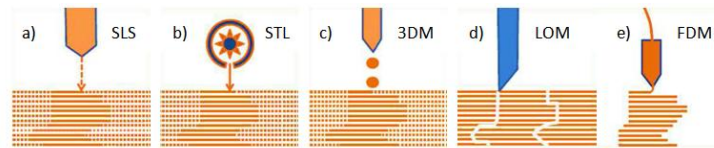


Fig. 2 Additive manufacturing [4]

The printer described in this work creates parts based on the Fused Deposition Modeling procedure. At this procedure a thermoplastic material will be heated and constantly pressed through one or more nozzles. The thermoplastic material cools down on the part surface by thermal conduction; it consolidates and creates a combination with the material which was applied before. This procedure is suitable for material with low thermo-conductivity like wax and plastics. But it is currently not suitable for metal and ceramics due to the high melting temperature of these materials and the high amount of machine work which is a consequence thereof. The degree of accuracy of the thread supplied is limited by the diameter of the thread itself. The combination of the viscous material and the material, which is already solidified works only by squeezing new material onto the solidified material. By doing this the profile of the thread deforms to an elliptical shape and it overcomes the surface tension. As the thread has a beginning and an end there might come up optically non-attractive weld lines [5]. There are two different concepts for the structure of the printer. The Gantry-Design has a basic plate which contains a movable gantry taking the printer head. Drive belts and multiphase motors enable fast motions in x-y plane. In z-plane (height dimension) the basic plate is moved by a lead screw slowly. This construction has a high stiffness of the portal. Thus, it is less vulnerable to oscillations than the RepRap design. The RepRap Design has three vertical pillars on which an arm can move on and thus the printer head is guided. Thus, the inertness of the moving parts of the printer is lower and enabling to work with higher printing speed.

III. FINITE ELEMENT METHOD

The aim of the finite-elements-method (FEM) is to depict the reality of a system on a digital simulation model [6-9]. The real system is reflected by a numerical computation. A precisely analytical computation is only doable for simple geometry like the cantilever, torsion rods or tensile rods if the constraints are selected precisely. As the parts are mostly more complex in practice the FEM and its approximation are applied by accepting the involved mistakes. The analytical calculation can support the validation of the FEM results. In the FEM the complex geometry is defined by linking of many small elements - the finite elements. Each element is defined by knots and rods. In the case of a mechanical strain of a part the exerting power is transmitted to the knots. For each knot it can be defined $F=k*\Delta u$, whereby F describes the exerting power, u describes the shifting of knots and k describes the stiffness of the rods. The summary of all equations of all knots is realized by a matrix shaped linear system of equations. The description rods between the knots can be done either in a linear or quadratic way. When using quadratic rods a third knot has to be implemented in the rod. In case of a deformation of the knot – rod net (mesh) the deformation can be depicted more precisely. A quadratic approach is connected with longer computation time – but it is mostly applied in practice. Thus, there are two methods to improve the results of FEM computation. By the h-version the diameter of the elements will be minimized whereby more elements are required assuming the part size remains constant. Thus an extra fine net is created. By the p-version the order of polynomial function will be increased.

IV. SIMULATION

The provision of simulation was divided into two areas. In the first part some investigations of trends were made. In this case the inner diameters d_{in} (Fig. 3 b, c, d, e, f) and the number of fins n (Fig. 3 g) were manually varied. Thereby the part was created in Inventor 2016, saved as step.-file, loaded in Ansys Workbench and simulated as thermal-static-analysis. In Fig. 3 you can see the different geometrics of the investigation of trends,

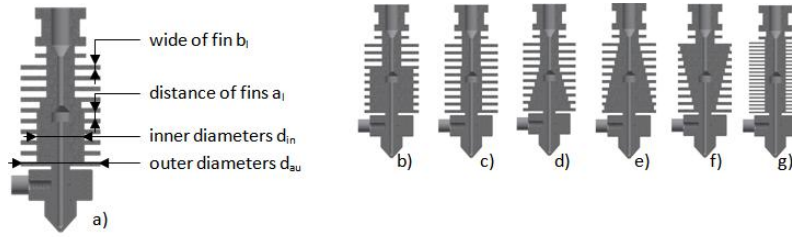


Fig.3 Buildsand parameters for the investigation of trends of the printer head

The aim of this procedure was to find out which parameters have the strongest qualitative influence on the cooling effect. With the findings of the first part of the investigation, the optimization of the second part of the investigation was started. The optimization consists of the thermal static analysis and the response surface optimization. The parts were created by Ansys itself, because the algorithm of the parameters in STEP-file cannot be changed. The distance of fins a_1 , the wide of fins b_1 as well as the number of fins n (Fig. 3 c) were varied. In Fig. 4 you can see the components of parts, measure points and the thermal conditions. It was assumed, that the hotpin has a temperature of 240°C and that it transfers this energy by 100% to the block of aluminum without losses. The hotpin and the extruder were still used in the investigation of trends, but during the optimization both parts were omitted, so that the simulation model is simplified. By doing so the simulation does not take long time. Through convection and radiation, the printer head emits energy to the environment. The complete outer surface of the printer head acts as the total surface of emitting energy by convection and radiation (Fig. 4c, d). The environmental temperature is 22°C.

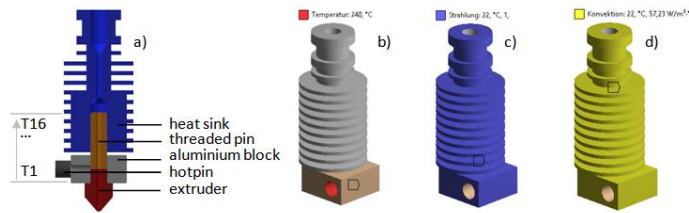


Fig. 4a) components of printer head and temperature measuring points b), c), d) thermal boundary conditions

For the calculation of the temperature reduction through convection, the heat transfer coefficient is required. The coefficient was determined analytically. The input variables are shown in Table 1. It was expected that the heat sink is a cylinder with a size of $l=0,04\text{m}$ and a diameter of $d=0,016\text{m}$. The cylinder will be blown perpendicularly to the circumferential surface with air and an airspeed of $v=100\text{ mm/s}$. (normal speed of RepRap printer). For the purpose if there is turbulent flow or laminar flow, the Reynolds-number was calculated.

$$Re = \frac{v \cdot l}{\nu} = 2,58 \cdot 10^{-4} < 2300 \tag{1}$$

The Reynolds number is smaller than 2300, hence there is laminar flow in this system. For the calculation of the heat transfer coefficient, the NuBelt number is required. This can be solved with the following formula on condition that $Re < 10$ and $0,6 < Pr < 1000$.

$$Nu = 0,664 \cdot Re^{0,5} \cdot Pr^{0,3} \cdot k = 9,64 \cdot 10^{-3} \tag{2}$$

The calculated value for the heat transfer coefficient only slightly deviates from the typical value of the aluminum heat transfer coefficient and air $\alpha=50\text{ W}/(\text{m}^2 \cdot \text{K})$ indicated by the literature.

$$\alpha = \frac{Nu \cdot \lambda}{l} = 57,23 \frac{W}{m^2 \cdot K} \tag{3}$$

Table 1. input variables for the calculation of the heat transfer coefficient

	$v \left[\frac{mm}{s} \right]$	$\lambda_{Al} \left[\frac{W}{m \cdot K} \right]$	$\nu \left[\frac{m^2}{s} \right]_{(22^\circ\text{C, air})}$	$l \text{ [m]}$	$K [-]_{\text{fluid}}$	$Pr [-]$
Value	100	237,5	15,5	0,04	1	0,714

The geometry of the different kinds of heat sink from the optimization (part 2) are shown in Fig. 5

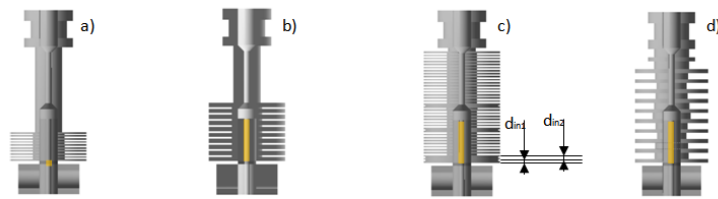


Fig. 5 Geometry for a minimal temperature after the simulation was finished

The following section shows the settings of the response surface optimization. At the beginning the design variables (input), such inner diameter, wide of fins or distance of fins, were set as variables in “DesignModeller” and “Mechanical”. Then the response surface optimization was linked with thermal analysis and the range of values for the design variables were set in the field “Design of Experiments” (DOE) (Table 1). The limitations of the range of values result from geometrical restrictions.

Table 2. Range of value for the design variables

	inner diameter d_{in} [mm]	outer diameter d_{au} [mm]	distance of fins a_1 [mm]	wide of fins b_1 [mm]
initial value	15	25	2	1,3
from	10	25	0,5	0,5
until	24	25	2,5	1,5

After this the setting “design of experiments type” was changed to “central composite design“ and “design type” was changed to “face-centered“, and the DOE-table was created. In the field “response surface” the settings “preserve design points after DX run“ and “retain files for preserved design points“ were activated [10]. In the field “optimization”, the algorithm “MOGA” (Multi-Objective Genetic Algorithm) was selected. With “MOGA” it is possible to have several targets and several boundary conditions and in this way it can reach a global optimum with continuous parameters. Therefore, this algorithm is most suitable for the task of this study. The input variables, which result in lowest temperature, were selected for the “DesignModeller” automatically. The area in the inner pipe of the threaded pins, where the algorithm should find the lowest temperature, is shown in Fig. 5 (orange area).

V. RESULTS AND DISCUSSION

Figure 6 and 7 show the time-independent temperature profile of the investigation of trends and the optimization of the heat sink. Thereby the temperature measure points are measured with the same distance from each other in the interior area of the pipe in the threaded pin (Fig. 6 a). The dotted line in Figure 6 represents the optimum temperature distribution. Thereby the aluminum block should have a temperature of 240°C, so that the materials liquefy itself. The aim is that the heat sink realizes a lower temperature than 70° as close as possible to the heat-break (Fig. 1) but not in the aluminum block. The geometry, which best fulfills the requirements, is the most suitable construction of heat sink. Figure 6 shows that all heat sinks have the same temperature from T1 until T5. This demonstrates that the heat sink does not have any thermal influence on the aluminum block and extruder. In the temperature transition area (near heat-break) T6-T9 some differences in the temperature are visible. Geometry g (Fig. 3) with twice number of fins and therefore with a higher surface and shows a lower offset of temperature in Figure 6 a. Thereby this geometry has the lowest temperature in T10-T16 (over heat-break) from all geometrics of the investigation of trends. The second best geometry is variant c. They have 10 fins and a normal distance of fins of $a_1=2$ mm and a wide of fins by $b_1=1,3$ mm like the initial geometry, but the inner diameter d_{in} is the lowest. The third best geometry is the initial geometry (Fig. 6 a) with a middle inner diameter d_{in} . All the others geometrics with higher inner diameter (Fig.3b) or changeable inner diameter do not have benefits. Thereby it was assumed at the beginning that a material accumulation near the heat-break leads to a better heat conduction and thereby the temperature is lower in the heat-break. This can be excluded. It is therefore to conclude that the maximizing of the surface of the heat sink by radiation through a high number of fins has a greater influence on the temperature distribution than a better heat conduction by material accumulation.

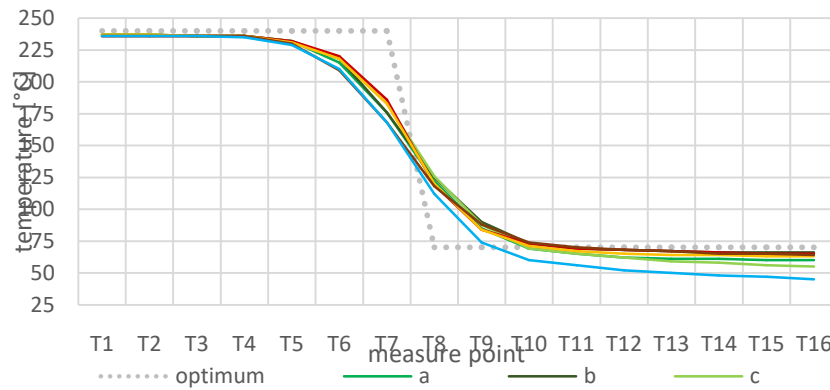


Fig. 6 Temperature profile by the investigation of trends

In the second portion of the study was realized an automatic optimization of the heat sink. The results are shown in Figure 5. Thereby the inner diameter and the numbers of fins were kept at a constant level by a) and b). Only the distance of fins and the wide of fins were varied by the algorithm. In comparison to b), at a) the algorithm is searching the target temperature at the heat-break and at b) the algorithm is searching the target temperature at the inner pipe of the threaded pin. It can be recognized immediately that the fins set near to the heat-break by a). Figure 7 shows that version b) has a lower temperature caused by thicker fins and greater surface in the area T10-T16 in comparison to a). The fins became thicker, because the target area is bigger (Fig. 5 b). In version c) there are used 30 fins instead of 10 fins, whereby the wide of fins and distance of fins are kept constant. But every single inner diameter should be changed (d_{in1} , d_{in2} ...) by the algorithm. It can be seen that every diameter has the lowest value of the value range (see Table 1), except d_{in1} , d_{in2} , d_{in11} , d_{in19} . Probably the material accumulation through the individual diameter acts as temperature maelstrom a speed up the heat conduction of the heat-break. But it can be confirmed, that the tripling of the number of fins and the increase of surface lead to the reduction of the temperature (Fig. 7 c). The last simulation d) should be highlighted particularly. Thereby only the individual inner diameter (10 fins) was changed systematically. The essential difference from version c) is that only d_{in1} to d_{in2} could be changed because of the high number of fins (more than 20) in version c) Ansys could not calculate with all parameters and switched off. It can be seen that the inner diameter has been kept constant and low by the algorithm. If the material is missing (Fig. 8, position A) the heat conduction cannot work so much and the result is that the inner diameter is bigger in this area. In this way the algorithm has been kept the heat flow stay constant over the amount of the part. Even in the second part of the study it was shown that, the best cooling effect is achieved by an increase of energy radiation through a high surface, or rather a high number of fins. A material accumulation through bigger fins l_b and lower distance of fins l_a is not conducive to reach the goal.

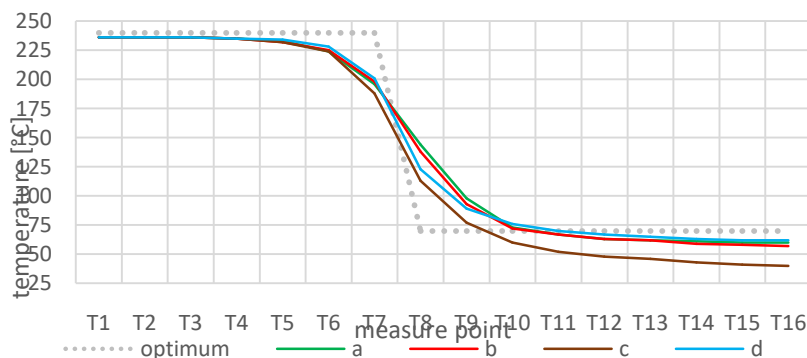


Fig.7 Temperature profile in the inner pipe of the threaded pin for the optimize geometry

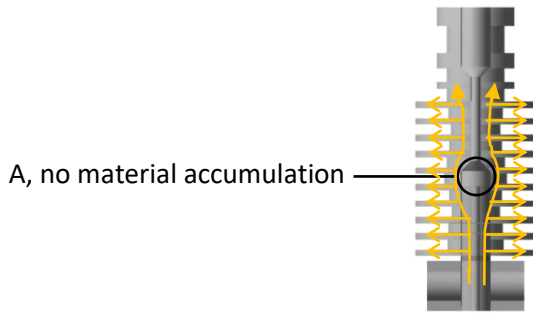


Fig. 8 Optimized geometry, version d(heat flow is marked orange)

VI. CONCLUSION

It can be concluded that the number of fins has the greatest influence on the cooling effect of the heat sinks, because this increases the surface. The inner diameter between the fins does not have any essential influence. The best geometry of the heat sink is given by a large number of fins and a small value for the inner diameter. Increased Heat conduction through material accumulation does not have essential effects to the cooling properties and therefore it can be neglected.

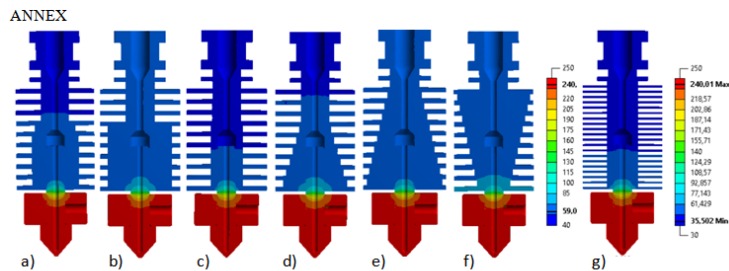


Fig. 9 Temperature in the cross-sectional area for all versions from the investigation of trends

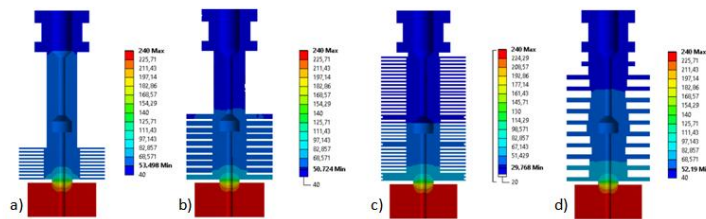


Fig. 10 Temperature in the cross-sectional area for all versions from the

REFERENCES

- [1] PrinterextruderApplicationBriefCase-Study, ANSYS, Inc, 2016 Additive Fertigung, Laser-Sintern Und Industrieller 3D Druck, Vorteile Und Funktionsprinzipien, Schriftenreihe Des IÖW 206/14, Berlin, 2014. Additive Fertigungsverfahren, 2014.
- [2] https://www.vdi.de/fileadmin/vdi_de/redakteur_dateien/gpl_dateien/vdi_statusreport_am_2014_web.pdf.
- [3] Tabellegenerativeverfahren-IHK
http://www.ihkoblentz.de/blob/koihk24/innovation/downloads/1479422/1a7c72b4e6d2930bb91b4c19badd5fde/uebersicht_additive_fertigungsverfahren-data.pdf

- [4] <https://www.kunststoffe.de/themen/basics/generative-fertigungsverfahren/extrusionsverfahren/artikel/extrusionsverfahren-fused-layer-modeling-flm-1057021.html>
- [5] FEM-Berechnung Für Maschinenbauingenieure, Klaus Fiegel, ISBN: 978-87-403-0313-1, 2013.
- [6] FEM Grundlagen Und Anwendungen Der Finiten-Elementen Methode Im Maschinen- Und Fahrzeugbau, 2010.
- [7] H.H.-Lee---Finite-Element-Simulations-With-ANSYS-Workbench-12, 12012.
- [8] Additive Fertigungsverfahren, Christian Pickert, Marco Wirth, 2013. ANDERS ANGANTYR, Constrained Optimization Of Rotor-Bearing Systems By Evolutionary Algorithms, Department Of Applied Physics And Mechanical Engineering, Division Of Computer Aided Design, Lulea University Of Technology, 2004.